CONF-840627--4

UCRL--90095

DE84 013336

Neutron and Gamma Dose and Spectra Measurements on the Little Boy Replica

Sharon Hoots and Don Wadsworth

Health Physics Annual Meeting, New Orleans, LA

June 1, 1984

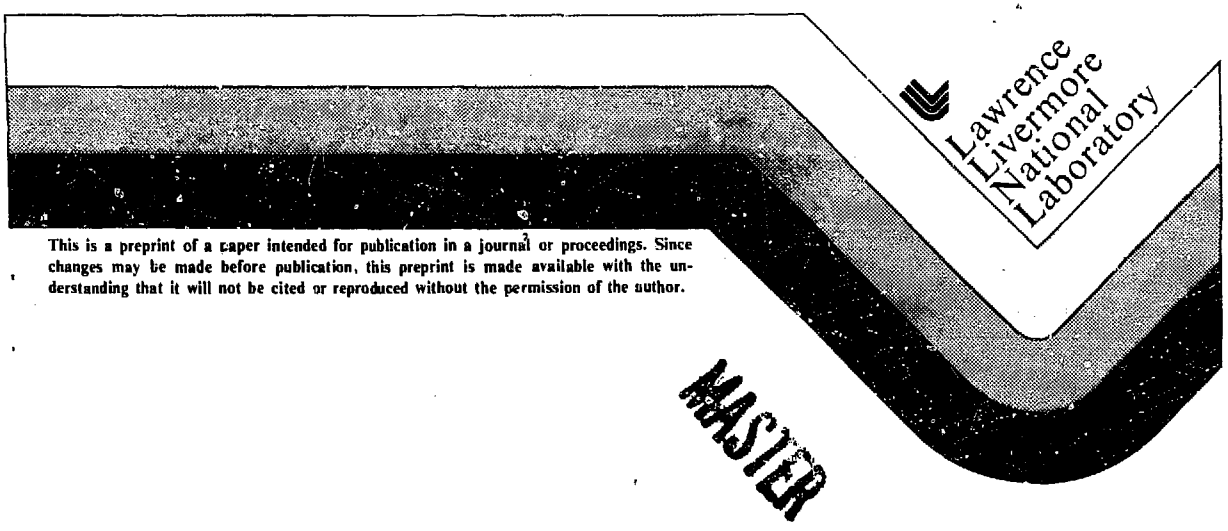

NEUTRON & GAMMA DOSE AND SPECTRA MEASUREMENTS ON THE LITTLE BOY REPLICA*

Sharon Hoots
Don Wadsworth

Weapons Engineering Division
Lawrence Livermore National Laboratory
Livermore, California 94550

ABSTRACT

The radiation-measurement team of the Weapons Engineering Division at Lawrence Livermore National Laboratory (LLNL) measured neutron and gamma dose and spectra on the Little Boy replica at Los Alamos National Laboratory (LANL) in April 1983. This assembly is a replica of the gun-type atomic bomb exploded over Hiroshima in 1945. These measurements support the National Academy of Sciences Program to reassess the radiation doses due to atomic bomb explosions in Japan. Specifically, the following types of information were important: neutron spectra as a function of geometry, gamma to neutron dose ratios out to 1.5 km, and neutron attenuation in the atmosphere. We measured neutron and gamma dose/fission from close-in to a kilometer out, and neutron and gamma spectra at 90 and 30 degrees close-in. This paper describes these measurements and the results.

---

* This work was performed under the auspices of the U.S. Department of Energy by LLNL under Contract No. W-7405-ENG-48.

DISCLAIMER

INTRODUCTION

Important information about the biological effects of ionizing radiation has been deduced from the study of the atomic bomb survivors. However, the accuracy of this information depends upon a knowledge of the actual dose each survivor received. Although dose and yield information from Fatman, exploded at Nagasaki, is well known; dose and yield information from Little Boy, exploded at Hiroshima, is not. Until recently, radiation output data from Little Boy have depended upon the 1965 evaluation by Auxier 'T65D'[1] that is assumed good to within 30%. Now, advanced methods for analyzing 'air-over-ground' neutron and gamma transport have led to new estimates which are significantly different. The two methods differ in computational technique, assumed-energy spectra, and amount of atmospheric attenuation. The validation of the computational technique has been discussed elsewhere.[2]

In an effort to validate the new energy spectra and atmospheric attenuation used in the calculations, scientists at the LANL constructed a replica of the gun-type Atomic Bomb (Little Boy) that was exploded over Hiroshima. A complete description of the replica is given elsewhere.[3] This replica was designed to be operated at various power levels so that a variety of neutron and gamma radiation measurements could be made near the replica. We and many other groups measured the neutron and gamma radiation from this replica during the year that it was operational. Our measurements included neutron spectra at two angles, gamma spectra at one angle, and neutron and gamma dose measurements at various distances.

MEASUREMENTS AND ENVIRONMENT

For most of our measurements, the assembly was moved out of doors and centered four meters off the ground in a nose-up vertical position. Neutron and gamma dose rate measurements were made close in at 0°, 30°, 60°, and 90° (90° is defined as horizontal). Figure 1 shows our neutron detector at 30° and 2.5 meters. Additional neutron and gamma dose rate measurements were made off the horizontal (90°) at 1, 2.5, 25.72, 198, 400, 600, and 900 meters with 9" spherical remmeters and gamma counter systems (both described in Appendix A). For distances beyond 2.5 meters, the detectors were supported on a truck at heights of up to 7.2 meters above the ground. Figure 2 shows our neutron detector supported on a truck. Although the purpose of the elevation was to avoid ground scatter, we saw no difference between elevated and ground level detectors. For the duration of the measurements, the temperature varied between 9 and 12°C, the pressure averaged 769 mbars, and the relative humidity was 40%.

Neutron spectral measurements were made with the Bonner Sphere and NE213 spectrometry systems (described in Appendix A). Due to time constraints, neutron spectral measurements were made only close in at 2.5 meters. We have complete neutron spectral measurements (consisting of both Bonner Sphere and NE213 data) at 30°, and NE213 spectra at 90°.

RESULTS

Our data are calibrated to power levels by run number and data supplied by LANL. Power-levels were specified relative to the linear current output

from the uncompensated ion chamber during the experiment. Table 1 lists the calibration data for our runs. The data are normalized to fissions/sec.

The neutron and gamma dose results are shown in Tables 2 and 3, respectively, and plotted in Fig. 3 as a function of distance. All readings are shown without spectral corrections. The energy response of the detectors used for dose measurement is discussed in the section on instrumentation.

The gamma to neutron dose rate ratio variation with distance is shown in Fig. 4. There is a large increase in the ratio with distance. Furthermore, Fig. 5 shows a geometric dose rate dependence. The measured dose rate at 0° is significantly lower than at 90°.

The neutron spectrum at 30° and 2.5 meters is shown in Fig. 6 -- this is a combined Bonner Sphere and NE213 spectrometer spectrum. Figure 7 shows a comparison between the NE213 neutron spectrum at 30° and 90°. The tabular data for all spectra are in Appendix B.

The NE213 spectrometer system records the energy spectrum from 0.5 MeV to 20 MeV. Since this range is a small part of the total neutron energy spectrum, we use the Bonner Sphere system to complete the spectrum. The agreement between the two systems is excellent.

DISCUSSION

The purpose of this work is to provide measurements that can be used to assess the validity of new calculational techniques. Specifically, we wanted to compare neutron spectra at various locations and angles, and to study neutron-attenuation in air. Soran[4] at LANL, using the same Monte Carlo code and cross sections as in the Hiroshima bomb calculations, calculated the neutron spectra emitted from the Little Boy replica at two distances and

several angles. Figures 8, 9 and 10 compare his calculations to our measurements. (We used 2.398 neutrons per fission[5] in our conversion of Soran's data). In Fig. 8 we compare our measurement at 30° and 2.5 meters to Soran's calculation at 22.5° and 2 meters (the closest comparison). At 90° we compare our high energy neutron spectrum (shown as the solid line in Fig. 9) to Soran's calculation at 90°. In both cases the effect of the difference in distance is minimal. Figure 10 shows a comparison of the high energy portion of spectra at 90° and 30°. Above 3 MeV our statistics are too poor to be shown here. All three figures show excellent agreement between calculated and measured values. These results validate the calculational technique used in the LANL neutron spectra calculations.

In order to make measurements to support the assessment of neutron and gamma transmission and attenuation in air, we made dose measurements at horizontal distances out to a kilometer. Experimental neutron dose rate measurements are typically given in terms of dose equivalents (mrem), while earlier A-Bomb survivor data are given in terms of tissue-kerma or free-field kerma. To make useful dose comparisons between experimental measurements and calculations one set of units must be converted to the other. Conversion presents a dilemma because neutron dose measuring instruments are designed to measure dose equivalent based upon the very factors which are sought, namely the quality factors for neutron radiation. (The response is built into the instruments). To convert the neutron-instrument reading to free-field kerma, the distribution of neutrons must be known at each and every data point.

We do not have neutron energy spectra at every data point. We do, however, have neutron energy spectra at 2.5 meters from the center of the replica. Folding these measured spectra with the kerma values for the ICRP standard man,[6] we calculated the total neutron kerma at 2.5 meters and 30°

to be 9.0×10^{-16} rads/fission. Comparing these values to the dose measuring instrument response at the same positions yields an instrument-response-to-kerma correction factor of 8.8 for the neutron remmeter. We have applied this correction factor to data from the neutron dose measuring instruments. No correction factors have been applied to the gamma dose measuring instrument readings that are in terms of milli-Roentgens.

The spectra change as distance from the replica increases due to air attenuation and scattering. We have assumed that the change in spectra will not change the correction factor significantly; the validity of this assumption must be studied in greater detail.

Figure 11 shows the measured neutron and gamma kerma (rads) variation with distance from the center of the replica normalized to a 15 kton total yield. (In the conversion to total kerma, we used 1.45×10^{23} fissions/kton).[7] Using our data we calculated neutron and gamma relaxation lengths to be about 160 and 250 meters, respectively. These values were determined from the kerma between 200 and 400 meters.

Figures 12 and 13 show the measured kerma variation with distance from the center of the replica. Also shown are values calculated by Loewe[8] at LLNL, using the same techniques as for the Little Boy calculations. The good agreement validates the methods used to calculate air transport for neutrons and gammas. In addition, the gamma/neutron dose rate ratio (shown in Fig. 4), increases at greater distances. This increase is caused by the higher decrease in neutron dose rate compared to the gamma dose rate. The neutrons have a shorter path in air than do the photons. The radiation output as a function of geometry around the replica was of interest also. The neutron measured dose/fission was found to be about four times larger at 90° than at 0°. The gamma measured dose/fission was found to vary similarly by a factor

of about three. Some variation is produced by the differences in material type and thickness that the radiation must penetrate -- there is more heavy material at 0° than at 90°. Other variations are produced by changes in spectra with angle and by a higher scatter component closer to the ground level (90°).

CONCLUSION

Our measurements were made to support the reassessment of radiation dose due to the atomic bomb explosions. Specifically, we wanted evidence to support or counter the predictions of the new calculational methods. Our results showed that the measured neutron spectra compare favorably at 30° and 90° to the spectra calculated by LANL. Furthermore, we showed that the neutron and gamma dose rates vary with position around the replica. Finally, we found that our neutron and gamma kerma values compare well with those calculated by LLNL. Since both calculations were made for the replica using the same codes and constants, our results provide evidence to support the new calculational methods.

ACKNOWLEDGMENTS

We extend a very special thanks to Dick Malenfant at LANL whose effort and interest made the Little Boy replica measurements a reality. We also thank the many employees of Q-2 at LANL who took the time and effort to assist us in our measurements. A final thanks goes to Don Goldman and W. E. Loewe at LLNL, who reviewed this work and provided helpful suggestions to the authors.

Table 1. Calibration data.

Run #	BF_3 Moderated (cpm)	Cd covered BF_3 (cpm)	Uncompensated ion chamber (cpm)	Linear digitized percent of scale	Fissions/sec
2				77% 10^{-10}	1.13 x 10^8
3				26% 10^{-9}	4.91 x 10^8
4	7.64 x 10^5	2124	4564	25% 10^{-9}	4.88 x 10^8
5	7.41 x 10^5	2067	4586	25-26% 10^{9}	4.91 x 10^8
6	7.53 x 10^5	2053	4515	25-26% 10^{9}	4.83 x 10^8
7	7.43 x 10^5	2070	4496	25% 10^{-9}	4.81 x 10^8
11	7.54 x 10^5	2100	4514	26% 10^{-9}	4.83 x 10^8
12	2.20 x 10^6	6900	13160	75% 10^{-9}	1.40 x 10^9
13	6.31 x 10^6	20700	4017	22.5% 10^{-8}	4.51 x 10^9
14	6.23 x 10^6	19300	3959	22.5% 10^{-8}	4.44 x 10^9
15	6.17 x 10^6	19300	3918	22.5% 10^{-8}	4.39 x 10^9
16	6.36 x 10^6	19700	4012	22.5% 10^{-8}	4.50 x 10^9
17	6.23 x 10^6	18602	3961	22.5% 10^{-8}	4.44 x 10^9
18	6.15 x 10^6	18393	3950	22.5% 10^{-8}	4.43 x 10^9
19	6.12 x 10^6	18221	3950	22.5% 10^{-8}	4.43 x 10^9
20	6.23 x 10^6	18828	3978	22.5% 10^{-8}	4.46 x 10^9
22	1.73 x 10^6	6148	13571	77% 10^{-9}	1.45 x 10^9
23	2.38 x 10^6	6670	14557	83% 10^{-9}	1.56 x 10^9
24	2.39 x 10^6	6517	14767	83% 10^{-9}	1.58 x 10^9
25	2.39 x 10^6	6685	14777	83% 10^{-9}	1.58 x 10^9
26	2.41 x 10^6	6790	15010	83% 10^{-9}	1.61 x 10^9
27	2.40 x 10^6	6695	14848	83% 10^{-9}	1.59 x 10^9
28	2.39 x 10^6	6698	14808	83% 10^{-9}	1.58 x 10^9
29	2.40 x 10^6	6727	14900	83% 10^{-9}	1.59 x 10^9
30	2.37 x 10^6	6513	14653	83% 10^{-9}	1.57 x 10^9
31	2.38 x 10^6	6563	14731	83% 10^{-9}	1.58 x 10^9
32	2.39 x 10^6	6636	14870	83% 10^{-9}	1.59 x 10^9
33	2.34 x 10^6	6452	14598	83% 10^{-9}	1.56 x 10^9
34	1.75 x 10^6	69528	14668	83% 10^{-9}	1.57 x 10^9

Table 1. (Continued).

Run #	BF_3 Moderated (cpm)	Cd covered BF_3 (cpm)	Uncompensated ion chamber (cpm)	Linear digitized percent of scale	Fissions/sec
4/22 9:36 am	3.73×10^7	6.23×10^5		80% 10^{-7}	1.47×10^{11}
4/22 10:00am	3.74×10^7	1.9×10^6		24% 10^{-6}	4.37×10^{11}
4/22 10:59am	3.75×10^7	7.0×10^6		90% 10^{-6}	1.64×10^{12}
4/22 11:59am			15917	90% 10^{-6}	1.64×10^{12}
9/7				92% 10^{-10}	1.76×10^8
9/8				92% 10^{-9}	1.74×10^9

Table 2. Neutron dose rates.

	Run #	Distance meters (feet)	Dose rate (mrem/hr)	Normalized dose rate (mrem/hr) (10% 10^{-6} scale)	ssions/sec	mrem/fission
Off 90°						
	2	1 (3.28)	63	1.01×10^{5}	1.13×10^{8}	1.55×10^{-10}
	3	1 (3.28)	210	7.78×10^{4}	4.91×10^{8}	1.19×10^{-10}
	4	1 (3.28)	195	7.51×10^{4}	4.88×10^{8}	1.11×10^{-10}
	11	2.5 (8.2)	33.6	1.24×10^{4}	4.83×10^{8}	1.93×10^{-11}
	12	2.5 (8.2)	99.5	1.28×10^{4}	1.40×10^{9}	1.97×10^{-11}
	13	2.5 (8.2)	318	1.30×10^{4}	4.51×10^{9}	1.96×10^{-11}
	11	25.72 (84)	0.46	1.74×10^{2}	4.83×10^{8}	2.65×10^{-13}
	25	25.72 (84)	1.45	1.68×10^{2}	1.58×10^{9}	2.55×10^{-13}
	12	25.72 (84)	1.42	1.82×10^{2}	1.40×10^{9}	2.82×10^{-13}
	17-20	25.72 (84)	4.76	1.99×10^{2}	4.44×10^{9}	2.98×10^{-13}
	4/22 9:36am	198 (650)	1.35	1.67	1.47×10^{11}	2.55×10^{-15}
	4/22 10:00am	400 (1312)	0.28	0.12	4.37×10^{11}	1.78×10^{-16}
	4/22 10:59am	600 (1969)	0.07	0.008	1.64×10^{12}	1.19×10^{-17}
	4/22 11:59am	900 (2953)	ND	ND	1.64×10^{12}	ND
Off 60°						
	5	1 (3.28)	141	5.32×10^{4}	4.91×10^{8}	7.98×10^{-11}
	14	2.5 (8.2)	240	9.8×10^{3}	4.44×10^{9}	1.50×10^{-11}
Off 30°						
	6	1 (3.28)	56.2	2.13×10^{4}	4.83×10^{8}	3.23×10^{-11}
	15	2.5 (8.2)	124.2	5.07×10^{3}	4.39×10^{9}	7.86×10^{-12}
	26-33	2.5 (8.2)	35.7[a]	4.19×10^{3}	1.59×10^{9}	6.23×10^{-12}

Table 2. (Continued).

Run #	Distance meters (feet)	Dose rate (mrem/hr)	Normalized dose rate (mrem/hr) (10% 10^{-6} scale)	Fissions/sec	mrem/fission
Off 0°					
7	1 (3.28)	53.4	2.06×10^{4}	4.81×10^{8}	3.08×10^{-11}
16	2.5 (8.2)	81.96	3.35×10^{3}	4.50×10^{9}	5.06×10^{-12}

[a] Measurements made using the Bonner Sphere technique.

Table 3. Gamma dose rates.

	Run #	Distance meters (feet)	Dose rate (mR/hr)	Normalized dose rate (mR/hr) (10% 10^{-6} scale)	Fissions/sec	mR/fission
Off 90°						
	7	1 (3.28)	1.02	3.92×10^{2}	4.81×10^{8}	5.89×10^{-13}
	16	1 (328)	9.49	3.87×10^{2}	4.50×10^{9}	5.86×10^{-13}
	17	2.5 (8.2)	1.75	7.14×10^{1}	4.44×10^{9}	1.09×10^{-13}
	22	25.72 (84)	0.032	3.36	1.45×10^{9}	6.13×10^{-15}
	25	25.72 (84)	0.02	2.32	1.58×10^{9}	3.52×10^{-15}
	4/22 9:36am	198 (650)	0.067	0.083	1.47×10^{11}	1.27×10^{-16}
	4/22 10:00am	400 (1312)	0.023	0.010	4.37×10^{11}	1.46×10^{-17}
	4/22 10:59am	600 (1969)	0.013	0.014	1.64×10^{12}	2.20×10^{-18}
	4/22 11:59am	900 (2953)	0.002	0.0002	1.64×10^{12}	3.39×10^{-19}
Off 60°						
	6	1 (3.28)	0.80	3.02×10^{2}	4.83×10^{8}	4.60×10^{-13}
	15	1 (3.28)	7.19	2.93×10^{2}	4.39×10^{9}	4.55×10^{-13}
	18	2.48 (8.2)	1.44	5.88×10^{1}	4.43×10^{9}	9.03×10^{-14}
Off 30°						
	5	1 (3.28)	0.37	1.4×10^{2}	4.91×10^{8}	2.09×10^{-13}
	14	1 (3.28)	3.38	1.38×10^{2}	4.44×10^{9}	2.11×10^{-13}
	19	2.5 (8.2)	0.84	3.43×10^{1}	4.43×10^{9}	5.27×10^{-14}

Table 3. (Continued).

Run #	Distance meters (feet)	Dose rate (mR/hr)	Normalized dose rate (mR/hr) (10% 10^{-6} scale)	Fissions/sec	mR/fission
Off 0°					
4	1 (3.28)	0.34	1.31×10^{2}	4.88×10^{8}	1.94×10^{-13}
11	1 (3.28)	0.32	1.19×10^{2}	4.83×10^{8}	1.84×10^{-13}
12	1 (3.28)	0.98	1.26×10^{2}	1.40×10^{9}	1.94×10^{-13}
13	1. (3.28)	3.2	1.30×10^{2}	4.51×10^{9}	1.97×10^{-13}
20	2.5 (8.2)	0.68	2.77×10^{1}	4.46×10^{9}	4.24×10^{-14}

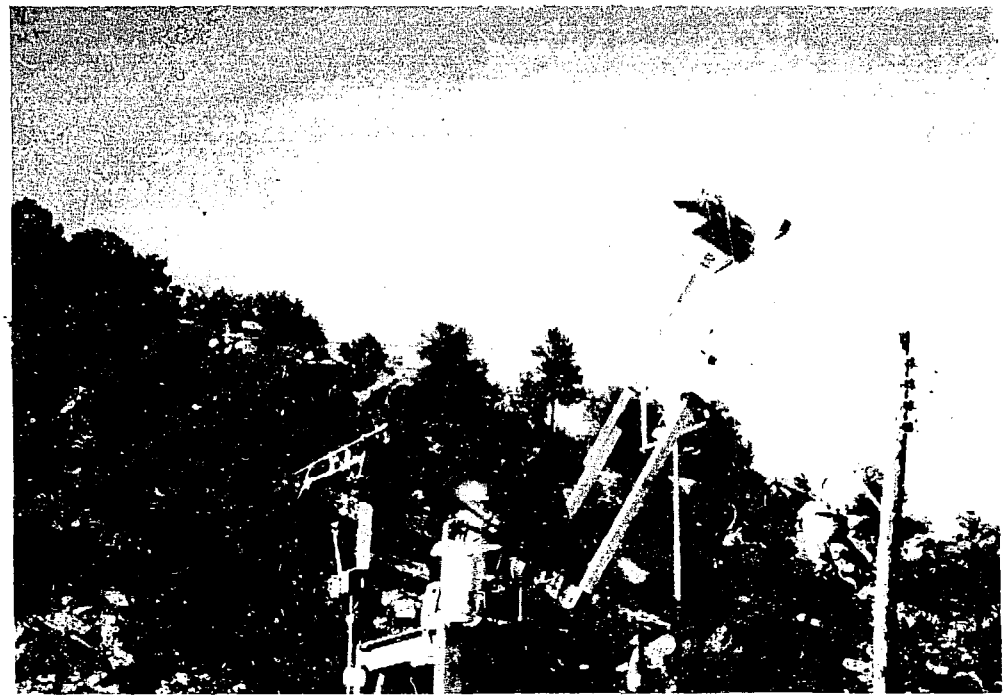

Figure 1. On-site neutron and gamma detectors.

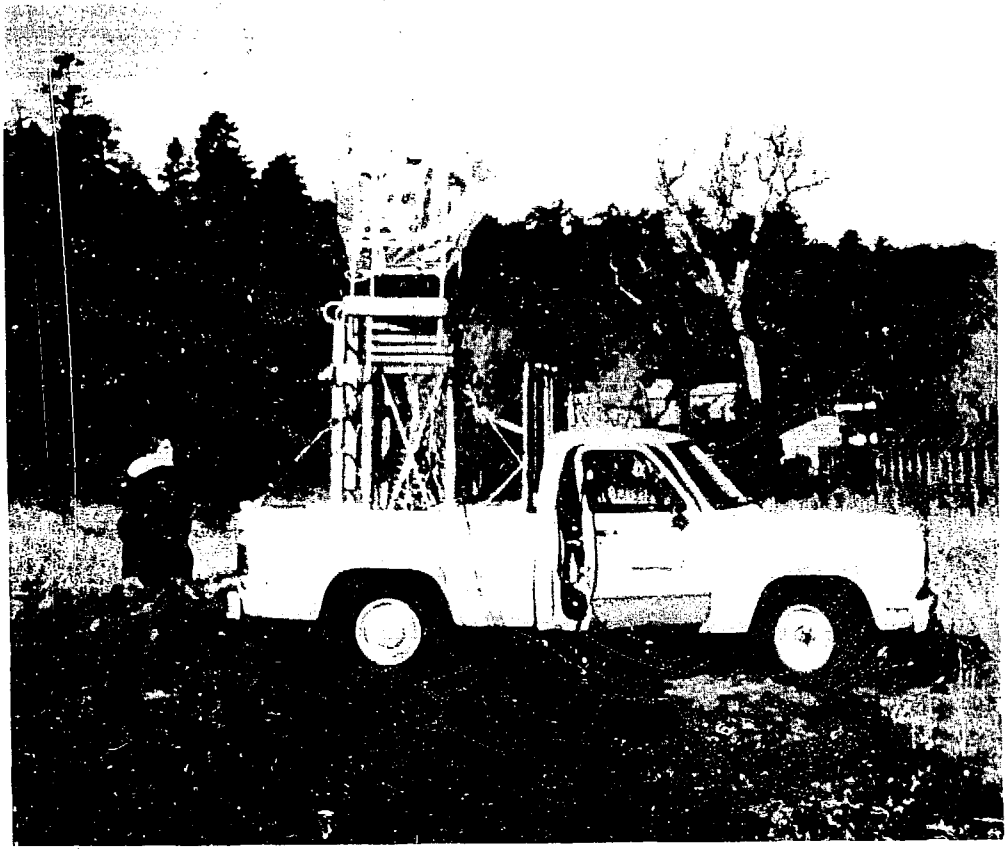

Figure 2. Little boy replica and neutron detector at 30° and 2.5 m.

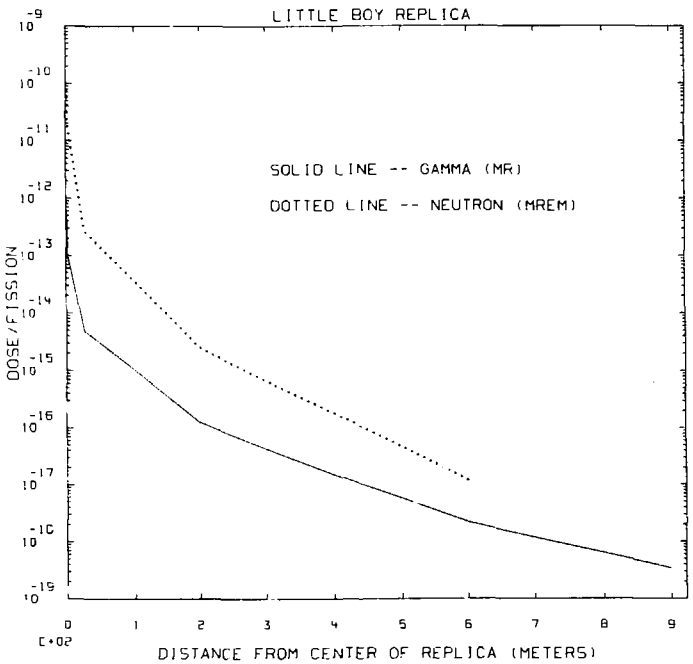

Figure 3. Variation in neutron and gamma dose rate with distance from the replica.

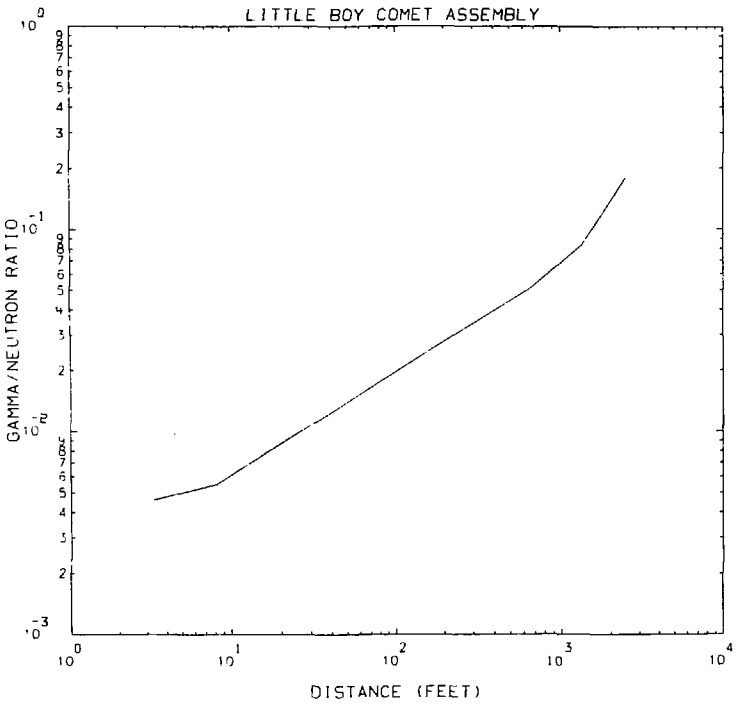

Figure 4. Variation in gamma/neutron ratio with distance from assembly.

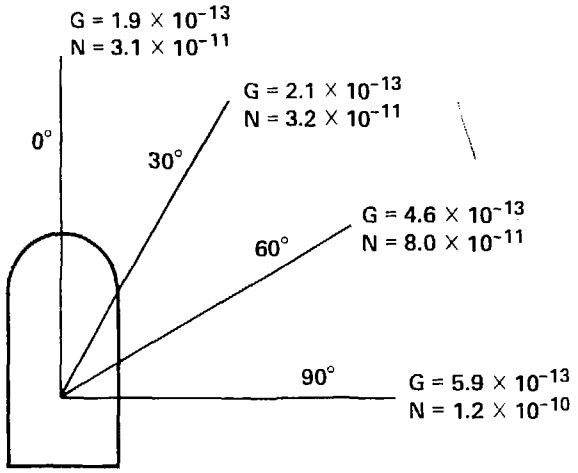

(a) 1 meter from center of replica

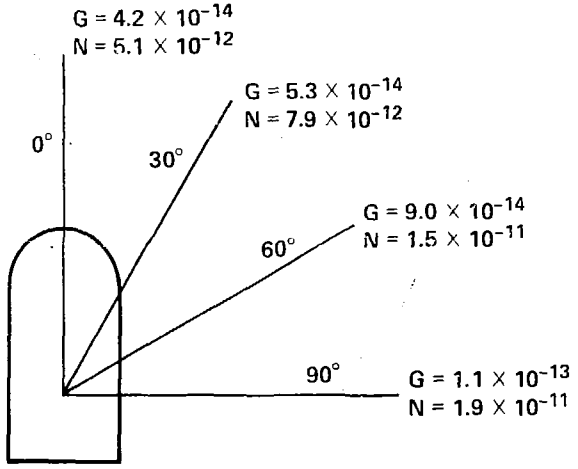

(b) 2.5 meters from center of replica

Figure 5. Gamma and neutron measured dose rates as a function of angle (mrem/fission - neutron, mR/fission - gamma).

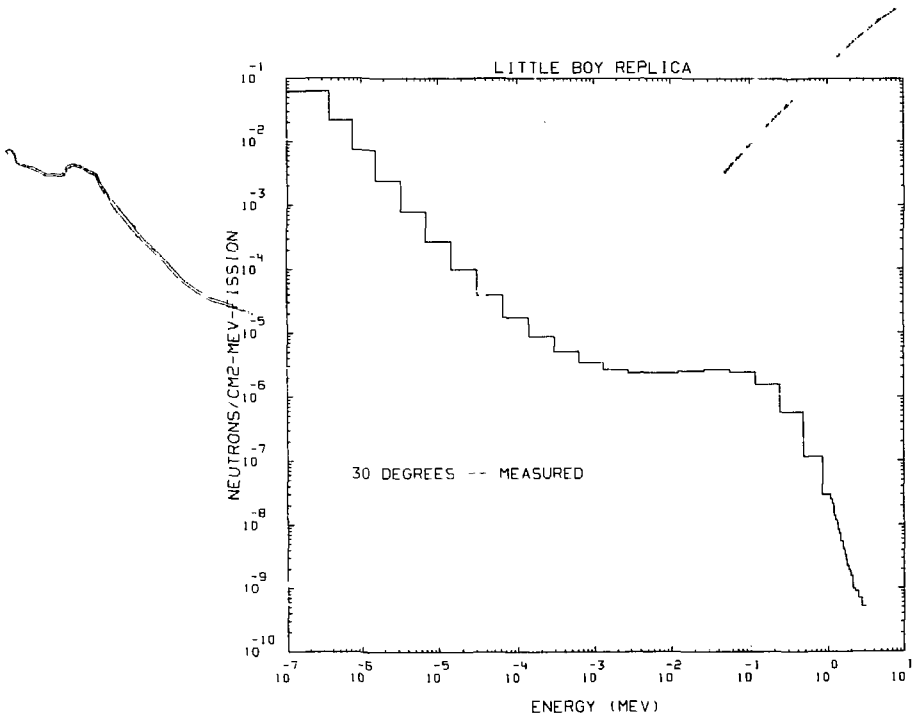

Figure 6. Neutron spectrum (combined Bonner Sphere and NE213 spectroscopy system results).

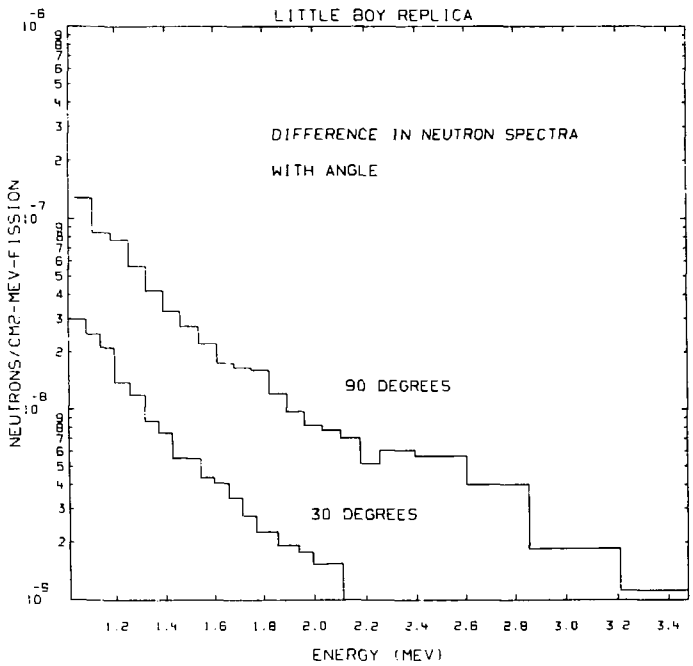

Figure 7. Comparison of neutron spectra at 30° and 90°.

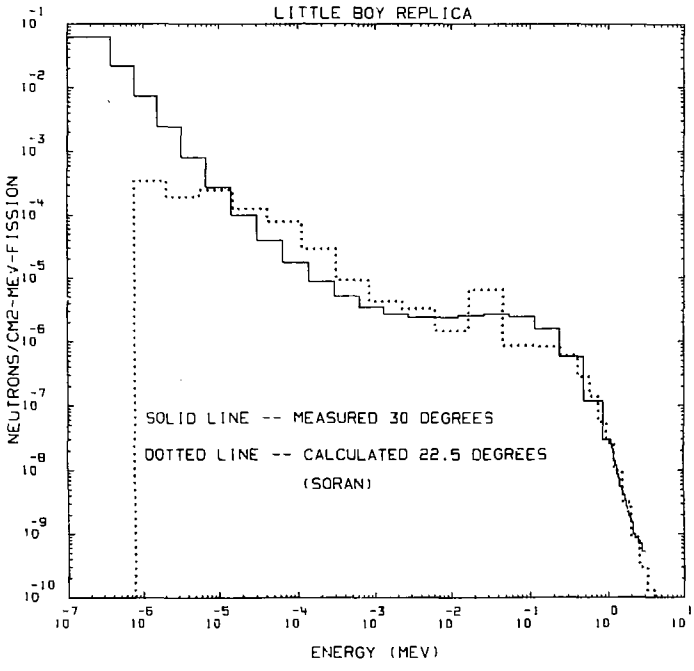

Figure 8. Comparison of the Little Boy replica measured neutron spectrum to the calculated neutron spectrum.

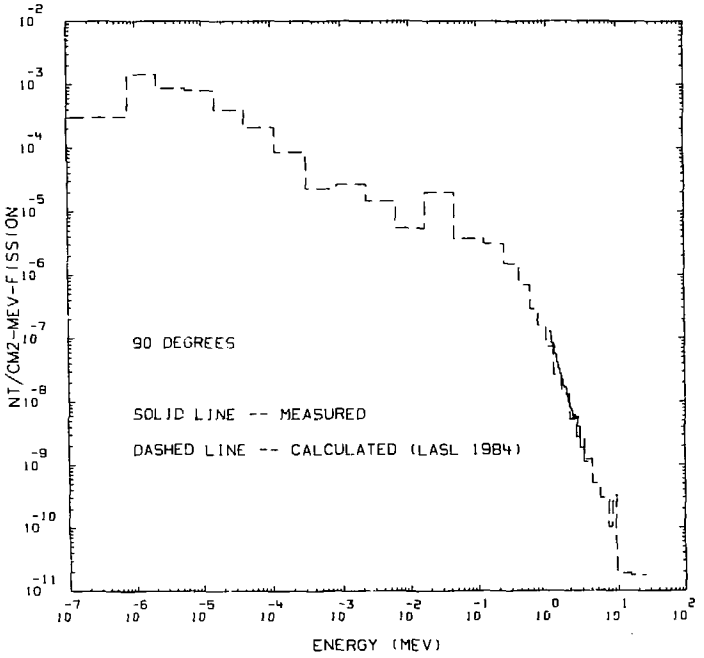

Figure 9. Comparison of the Little Boy replica neutron spectrum at 90°.

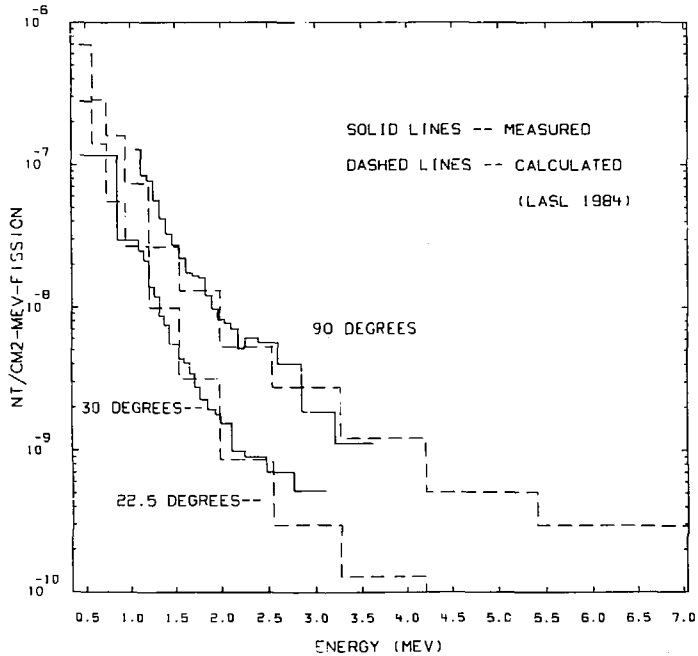

Figure 10. Comparison of the Little Boy replica neutron spectra above 1 MeV.

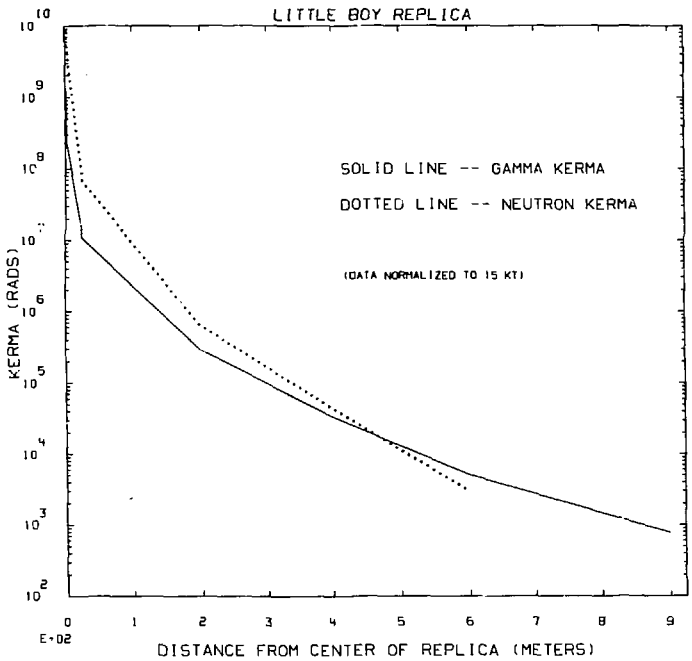

Figure 11. Measured kerma variation with distance from the replica.

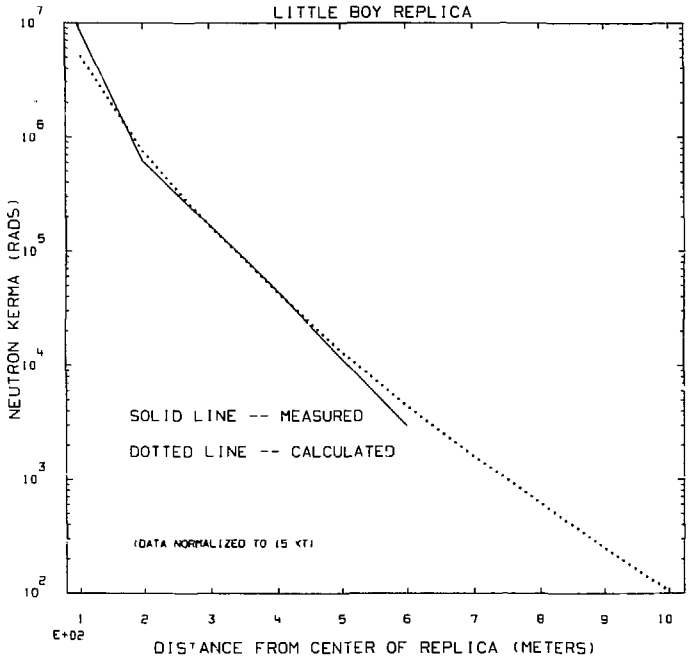

Figure 12. Neutron kerma variation with distance from the replica: a comparison between measured and calculated values.

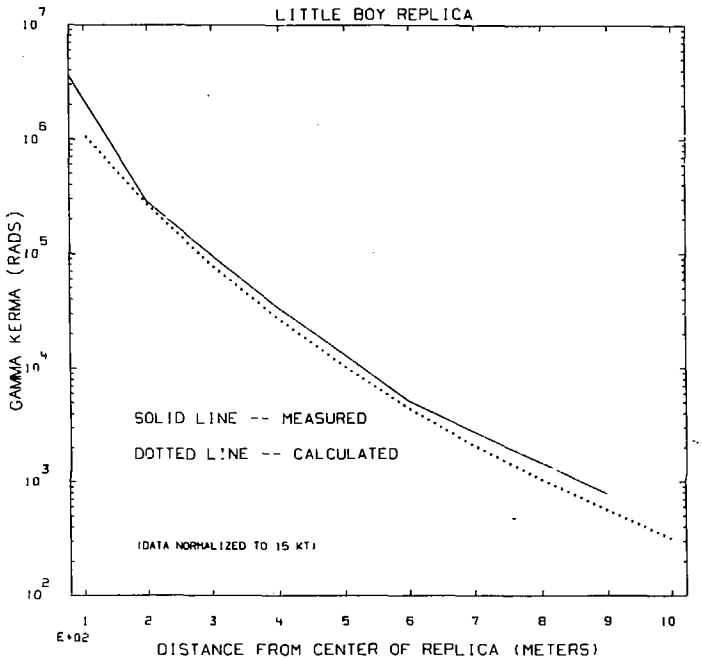

Figure 13. Gamma kerma variation with distance from the replica: a comarison between measured and calculated values.

APPENDIX A

INSTRUMENTATION

Neutron dose measurements were made with a modified spherical remmeter. Our detector consists of a 9-in diameter cadmium-loaded polyethylene sphere with a helium-3 tube in the center. This detector has an electronic system which allows us to operate in the pulse-counting mode. The helium-3 tube response is similar to the BF3 tube (i.e., they both respond similarly to the theoretical dose equivalent for neutrons over the energy range from 0.25 eV to about 10 MeV). However, because the helium-3 tube is at a higher pressure, it is more sensitive than the BF_3 by a factor of 6 to 8. This detector has an excellent gamma rejection also.

We convert from count rate to dose rate using a calibration factor in cpm/mrem/hr determined from exposures to a Cf-252 spectrum. Even though the detector response follows the theoretical dose equivalent for neutrons, the detector gives a higher count rate per mrem for intermediate energy neutrons than for fast neutrons (such as our calibration source). When measured spectra consist of neutrons in the intermediate energy range, adjustments should be made to the measured dose rate to compensate for this higher response. Spectral corrections were made to the data presented as described in this paper.

Gamma dose measurements are made using the HP-270 probe from Eberline. With the beta shield on the probe closed, the response of this detector is within + or - 10% of the actual exposure from 30 keV to 2000 keV. We use this detector in the pulse counting mode and calibrate to Cesium-137 gamma rays. Since high energy gamma rays were measured (> 2000 keV), a spectral

correction should be applied to these data. No corrections have been made in the data presented in this paper.

Neutron spectral measurements are accomplished by two methods: the Bonner Sphere and NE213 spectroscopy systems. The NE213 system consists of a 2-by-2-in. organic scintillator in conjunction with the PSD 5010 (Link Systems Limited, Halifax Road, High Wycombe Bucks HP12 3Se, England) pulse-shape discriminator.

Proton recoils produced by incident neutrons in the organic scintillator are identified by the Link pulse-shape discriminator through a charge integration and comparison process. The process has limitations in the low energy range, where the signal amplitude is not sufficient to perform discrimination. Also, since all events are analyzed, a count rate limitation, especially in high gamma background, is imposed. This system is used to obtain data above 500 KeV.

All signals from the photomultiplier tube are amplified with linear electronics. The multichannel analyzer is gated to accept only events identified as neutrons by the pulse shape discriminator.

A computer program (SHORTSPEC)[9] performs the unfolding process that determines the incident neutron energy from the pulse height data. In the code, curves that relate the scintillator light output to the proton recoil energy are used to determine the proton recoil distribution. A derivative unfolding process is used on the proton recoil distribution to arrive at the spectrum of neutrons.

The Bonner Sphere Spectroscopy method[10,11] involves the use of a 4-by-4-mm ^{6}LiI scintillation detector with a set of five polyethylene spheres and a cadmium sleeve. The spheres fit over the detector so that the detector is always in the center. The pulses from the detector are measured

in a portable multichannel analyzer where the pulses due to n-alpha interactions are identified. A set of seven counts--bare detector, cadmium-covered detector, and 3-, 5-, 8-, 10-, and 12-in. spheres--are compared in an iterative computer routine (BON) until a spectrum is found which best fits the data (determined by the method of least squares). Response functions are from Sanna.[12]

APPENDIX B

SPECTRAL TABULAR DATA

Table B1. Neutron spectrum at 30° and 2.5 m.

Energy (MeV)	nt/cm^2/MeV/fission
2.070E-07	6.240E-02
5.320E-07	2.176E-02
9.930E-07	7.359E-03
2.100E-06	2.434E-03
4.450E-06	7.988E-04
9.420E-06	2.724E-04
2.000E-05	9.875E-05
4.220E-05	3.919E-05
8.940E-05	1.742E-05
1.890E-04	8.806E-06
4.040E-04	5.120E-06
8.550E-04	3.447E-06
1.800E-03	2.680E-06
3.800E-03	2.378E-06
8.050E-03	2.365E-06
1.700E-02	2.516E-06
3.610E-02	2.654E-06
7.640E-02	2.428E-06
1.580E-01	1.572E-06
3.180E-01	5.762E-07
6.400E-01	1.164E-07
1.060E+00	2.960E-08
1.120E+00	2.490E-08
1.170E+00	2.120E-08
1.230E+00	1.390E-08
1.290E+00	1.190E-08
1.350E+00	8.690E-09
1.400E+00	7.520E-09
1.460E+00	5.540E-09
1.520E+00	5.520E-09
1.570E+00	4.370E-09
1.630E+00	4.100E-09
1.690E+00	3.420E-09
1.740E+00	2.760E-09

Table B1. (Continued).

Energy (MeV)	$n/cm^2/MeV/fission$
1.800E+00	2.270E-09
1.850E+00	1.920E-09
1.910E+00	1.930E-09
1.970E+00	1.780E-09
2.020E+00	1.540E-09
2.080E+00	1.550E-09
2.140E+00	9.890E-10
2.190E+00	6.940E-10
2.250E+00	5.800E-10
2.310E+00	7.060E-10
2.360E+00	9.010E-10
2.420E+00	7.000E-10
2.480E+00	4.310E-10
2.530E+00	7.190E-10
2.590E+00	7.030E-10
2.650E+00	7.230E-10
2.700E+00	1.190E-10
2.760E+00	2.150E-10
2.820E+00	1.580E-10
2.870E+00	4.500E-10
2.930E+00	5.210E-10

Table B2. Little Boy spectrum at 90° and 2.5 m (NE213 Spectometry system).

Energy (MeV)	$n/cm^2/MeV/fission$
1.764	1.627E-08
1.868	1.509E-08
1.973	1.070E-08
2.077	1.011E-08
2.181	9.639E-09
2.285	7.886E-09
2.389	7.709E-09
2.493	6.658E-09
2.597	6.544E-09
2.701	6.418E-09
2.806	5.710E-09
2.910	5.171E-09
3.014	5.109E-09
3.118	4.677E-09
3.222	4.616E-09
3.326	4.250E-09
3.430	4.213E-09
3.535	3.000E-09
3.639	2.266E-09
3.743	2.062E-09
3.847	1.651E-09
3.951	1.527E-09
4.055	1.259E-09
4.159	1.004E-09
4.264	1.011E-09
4.368	8.772E-10
4.472	7.570E-10
4.576	7.272E-10
4.680	6.500E-10
4.784	5.944E-10
4.888	5.814E-10
4.993	5.207E-10
5.097	4.780E-10
5.201	4.422E-10
5.305	4.318E-10
5.409	4.011E-10
5.513	3.772E-10
5.617	3.749E-10
5.722	3.544E-10
5.826	3.306E-10
5.930	3.080E-10
6.034	2.825E-10
6.138	2.746E-10
6.242	2.560E-10

Table B2. (Continued).

Energy (MeV)	$n/cm^2/MeV/fission$
6.346	2.289E-10
6.451	2.147E-10
6.555	2.018E-10
6.659	1.991E-10
6.763	1.879E-10
6.867	1.771E-10
6.971	1.603E-10
7.075	1.503E-10
7.180	1.419E-10
7.284	1.327E-10
7.388	1.232E-10
7.492	1.112E-10
7.596	9.430E-10
7.700	8.937E-10

REFERENCES

1. J. A. Auxier, Ichiban: Radiation Dosimetry for the Survivors of the Bombings of Hiroshima and Nagasaki, TID-27080, Technical Information Center, U.S. Energy Research and Development Administration, Oak Ridge, TN (1977).

2. W. E. Loewe and E. Mendelsohn, "Neutron and Gamma-Ray Doses at Hiroshima and Nagasaki," Nucl Sci Eng 81, 338 (1982).

3. R. E. Malenfant, "Little Boy Replication: Justification and Construction," Seventeenth Midyear Topical Symposium of the Health Physics Society, Pasco, Washington, Feb. 5-9 (1984).

4. P. Soran, Los Alamos National Laboratory, Los Alamos, NM, private communication (1984).

5. D. E. Cullen, et. al., An Integrated System for Production of Neutronics and Photonics Calculated Constants, Lawrence Livermore National Laboratory, Livermore, CA, UCRL-50400, vol. 16, Rev. 2 (1976).

6. M. S. Singh, Kerma Factors for Neutrons and Photons with Energies below 20 MeV, Lawrence Livermore National Laboratory, Livermore, CA, UCRL-52850 (1979).

7. J. A. Auxier, et. al., "Free-field Radiation-dose Distributions from Hiroshima and Nagasaki Bombings," Health Physics 12, 425-429 (1966).

8. W. E. Loewe, Lawrence Livermore National Laboratory, Livermore, CA, private communication (1984).

9. D. . Slaughter, D. W. Rueppel, and D. A. Fuess, Neutron Spectrum Measurements for Radiation Protection Purposes, Lawrence Livermore National Laboratory, Livermore, CA, UCRL-52415 (1978).

10. M. Awschalom, Use of the Multisphere Neutron Detector for Dosimetry of Mixed Radiation Fields, Princeton University, NJ.

11. R. L. Bramblett, R. E. [illegible]g, and T. W. Bonner, "A New Type of Neutron Spectrometer," Nucl Instrum Methods 9 (1960).

12. Robert S. Sanna, Thirty One Group Response Matrices for the Multisphere Neutron Spectrometer Over the Energy Range Thermal to 400 MeV, Health and Safety Laboratory, U.S.A.E.C., Washington, D.C., HASL-267 (1973).